ELSEVIER

Contents lists available at ScienceDirect

# **Environment International**

journal homepage: www.elsevier.com/locate/envint



# Full length article

# Exploring the relationship between the androgen receptor and structural configuration of benzophenones: a combination of computational analysis and laboratory models

Da-Hyun Jeong <sup>a</sup>, Rajesh Kumar Pathak <sup>b</sup>, Da-Woon Jung <sup>a</sup>, Jun-Mo Kim <sup>c,\*</sup>, Hee-Seok Lee <sup>a,d,\*</sup>

- <sup>a</sup> GreenTech-based Food Safety Research Group, BK21 Four, Department of Food Science and Biotechnology, Chung-Ang University, 4726 Seodong-daero, Anseong-si, Gyeonggi-do 17546, Republic of Korea
- <sup>b</sup> Pere Virgili Institute for Health Research, Tarragona 43005, Spain
- <sup>c</sup> Department of Animal Science and Technology, Chung-Ang University, 4726 Seodong-daero, Anseong-si, Gyeonggi-do 17546, Republic of Korea
- d Department of Food Safety and Regulatory Science, Chung-Ang University, 4726 Seodong-daero, Anseong-si, Gyeonggi-do 17546, Republic of Korea

#### ARTICLE INFO

Handling Editor: Adrian Covaci

Keywords:
Androgen receptor
Benzophenones
Molecular dynamics simulation
Molecular docking
Endocrine disruption

#### ABSTRACT

This study explored the interactions between benzophenones (BPs) and androgen receptors (AR) using computational and experimental approaches. BPs are potential endocrine disruptors that are commonly found in cosmetics, such as sunscreen. Molecular docking and molecular mechanics with generalized Born and surface area continuum solvation calculations revealed that dihydroxylation form of BP-1, BP-2 had higher binding affinities to AR compared with BP-1, BP-3. Key interactions with residues, such as Gln711 and Asn705, were identified. Density functional theory analysis revealed that BP-2 has a balanced energy gap, which contributes to its stability and reactivity. Cell-based assays validated these computational results, showing that BP-2 had stronger AR antagonistic effect than BP-1 and BP-3. Furthermore, BP-2 enhances the AR-mediated luciferase signal at specific concentration through inducing dimerization of cytosolic AR, whereas BP-1 and BP-3 had no AR agonistic effects. These changes in AR-mediated transcriptional activation activity were observed in flutamide and hydroxy-flutamide as well. As expected, changes in AR-mediated endocrine disrupting potential due to configurational modification of BP-1 to BP-2 by dihydroxylation resulted in whole AR protein expression. These findings suggest that BP-2 is a strong AR modulator and a potential endocrine disruptor, offering insights into how similar compounds may interact with AR.

# 1. Introduction

Endocrine-disrupting chemicals (EDCs) mimic the action of hormones within the body, interfering with normal processes involved in hormone synthesis, transport, metabolism, and secretion. Exposure to EDCs in the natural environment via different routes (La Merrill et al., 2020) can increase the risk of reproductive disorders (Axelstad et al., 2018; Johansson et al., 2017; Skakkebaek, 2016), cognitive impairments (Amano et al., 2018; Ghassabian and Trasande, 2018; Jefferson et al., 2018), metabolic disorders (Alonso-Magdalena et al., 2010; Cano-Sancho et al., 2017), and cancer (Heindel et al., 2017; Sifakis et al.,

2017; Giulivo et al., 2016; Scsukova et al., 2016). The endocrine system consists of glands that release hormones that act as chemical messengers to regulate various physiological functions, including growth, development, reproduction, energy balance, metabolism, and weight control (Larry Jameson and De Groot, 2016). EDCs primarily function by binding to nuclear hormone receptors, specifically estrogen receptor (ER) and androgen receptor (AR), with various reported mechanisms of action aimed at disrupting endocrine processes (Hong et al., 2002; Sakkiah et al., 2016).

Regarding biological role of AR in human body, AR is found in various tissues and plays a key role in regulating essential biological

E-mail addresses: junmokim@cau.ac.kr (J.-M. Kim), hslee0515@cau.ac.kr (H.-S. Lee).

<sup>\*</sup> Corresponding authors at: Department of Animal Science and Technology, Chung-Ang University, 4726 Seodong-daero, Anseong-si, Gyeonggi-do 17546, Republic of Korea (J.-M. Kim). GreenTech-based Food Safety Research Group, BK21 Four, Department of Food Science and Biotechnology, Chung-Ang University, 4726 Seodong-daero, Anseong-si, Gyeonggi-do 17546, Republic of Korea (H.-S. Lee).

processes, such as muscle growth, reproductive function, and development of the prostate and testes (Gelmann, 2002). This receptor interacts with endogenous ligands, such as testosterone and  $5\alpha$ -dihydrotestosterone (DHT), to translocate into the nucleus, bind to the Androgen Responsive Element (ARE), and control the transcription of crucial target genes involved in male sexual differentiation and development (Heinlein and Chang, 2004; Dayan Elshan et al., 2019).

AR is categorized within nuclear receptor subfamily 3 based on their structural and functional characterizations. The structure comprises three functional domains: an N-terminal domain (NTD), DNA-binding domain (DBD), and C-terminal ligand-binding domain (LBD), along with a hinge region linking the DBD and LBD (Gao et al., 2005; Davey and Grossmann, 2016). The AR regulates the activity of transcription factors through interactions at the AR N-terminal activation factor-1 (AF-1) sites within the DBD and the AR C-terminal activation factor-2 (AF-2) sites within the LBD. The AR LBD contains three active sites: a ligand-binding pocket (LBP), where AR ligands bind to alter the function of AR; an AF-2 site; and a binding function-3 site (BF-3) (Sakkiah et al., 2018).

With respect to AR-mediated endocrine disrupting potential by exogenous ligands, extensive research on the chemical properties of AR ligands has categorized these compounds as either agonists or antagonists based on their ability to stimulate or suppress the transcription of AR target genes (Azhagiya Singam et al., 2019). In addition to endogenous ligands, such as hormones and neurotransmitters, exogenous ligands including environmental chemicals, toxins, and pharmaceuticals, can disrupt the normal functioning of the AR. Several chemicals, including linuron, flutamide, and dicarboximide fungicides, such as vinclozolin and procymidone, cause toxicity through their action as AR antagonists (Lambright et al., 2000; Martinović et al., 2008; Zacharia, 2017; Serçinoğlu et al., 2021). These findings suggest that interference with the AR signaling pathway can lead to reproductive health issues, androgen-insensitive syndrome, and prostate cancer (Shtivelman et al., 2014; Matsumoto et al., 2013; Lonergan and Tindall, 2011).

Due to growing apprehensions regarding the adverse effects of EDCs, the Organization for Economic Cooperation and Development (OECD) has defined EDCs as mediators of estrogen, androgen, thyroid hormones, and steroid synthesis, and presented a conceptual framework consisting of Levels 1 to 5. Ongoing research aims to develop and validate testing methods that can be used at each stage (OECD, 2018). The United States Environmental Protection Agency (EPA) conducts a comprehensive assessments of the endocrine-disrupting potential of various chemical compounds through the Endocrine Disruptor Screening Program. The EPA is also currently concentrating on the development of predictive modeling methodologies aimed at identifying the endocrine-disrupting effects of chemical substances.

In terms of data ecosystem using non-animal test methods to assess the AR-mediatated critical effects of chemicals, recent studies have investigated ligand binding, structure, and activity prediction modeling of AR using molecular docking and molecular dynamics simulations (MDS). Androgens acting as AR agonists bind to LBP and interact with coactivators via AF-2, leading to structural changes in the LBD (Jin et al., 2019; Wahl and Smieško, 2018; Sakkiah et al., 2018). Other studies have identified specific amino acid residues (Arg725, Leu704, Leu705, Asn705, Gln711, and Thr877), emphasizing the importance of hydrogen bonding between the wild-type AR LBD and ligand in AR agonistic effects (Gao et al., 2005; Bohl et al., 2007; Tan et al., 2015). However, structural mechanisms governing the activity of AR antagonists, including environmental pollutants, have yet to be fully elucidated. Current findings indicate that when AR antagonists bind to LBP, they compete with AR agonists or directly interact with AF-2 or BF-3, inhibiting AR transcriptional activity through structural changes (Azhagiya Singam et al., 2019; Tan et al., 2015).

Typically, the Hershberger assay, a widely used *in vivo* short-term test, evaluates the androgenic or antiandrogenic activity of compounds by measuring changes in the weights of androgen-sensitive

tissues (e.g., ventral prostate, seminal vesicles, and LABC muscle) in castrated male rats (OECD TG 441). While this assay provides valuable insights into androgen receptor-mediated responses, its limitations—including the use of live animals and the complexity of *in vivo* environments—highlight the need for complementary approaches. As previously stated, computational approaches, such as molecular docking and MDS, play crucial roles in elucidating the relationship between structure and function in macromolecules (Hollingsworth and Dror, 2018; Hospital et al., 2015). Using computational approaches before laboratory experiments (*in vitro/in vivo* assays) can reduce costs and minimize the need for animal testing (Galli, 2014; Freires et al., 2017).

Structually, benzophenone (BP) is classified as an aromatic compound, with 2-hydroxybenzophenone derivatives benzophenone-1 (BP-1, 2,4-dihydroxybenzophenone) through Benzophenone-12 (BP-12); each compound displays different characteristics based on molecular substitutions (Heurung et al., 2014). BPs are commonly used as ultraviolet (UV) light absorbers, and their derivatives are commonly utilized in a variety of cosmetic products, including sunscreens, personal care products, paints, plastics, and pesticides, because of their photostabilizing properties. Furthermore, they have also been identified in aquatic environments (Negreira et al., 2009; Rodil et al., 2012). However, BPs may induce allergies and photoallergies (Du et al., 2017). BPs appear to interfere with the endocrine system, including estrogenic and androgenic functions. Typically, AR ligands are verified through binding assays or reporter gene analyses conducted in vitro, with varying outcomes observed across different studies. Kawamura et al. analyzed the estrogenic and antiandrogenic activities of 19 different types of BPs and their derivatives using a reporter gene assay. They identified that 17 compounds displayed AR antagonistic activity, with 2,2',4,4'-tetrahydroxybenzophenone (BP-2) being the most potent AR antagonist (Kawamura et al., 2003). Satoh et al. (2001) reported that 2-hydroxy-4methoxybenzophenone (BP-3) is a weak AR antagonist. However, Satoh et al. reported that BPs have no affinity for the AR, and Yamasaki et al. (2003) reported that some hydroxylated BPs do not act as antagonists in the Hershberger assay. Therefore, the function of the reporter genes of BPs and their derivatives has not been clearly elucidated, and the correlation between the structure and activity of the derivatives remains unknown.

This study aimed to investigate the structural variations in the endocrine-disrupting potentials of BP-1 and its derivatives (BP-2, and BP-3). We applied computational modeling to predict AR-mediated endocrine disrupting potential and the correlation between structure and binding affinity. Furthermore, the consistency of the outcomes of androgenic activity prediction modeling prediction was validated via cell-based assays.

## 2. Materials and methods

## 2.1. Ligand preparation

The structures of the BPs, hydroxyflutamide, and flutamide were obtained from the PubChem database and prepared using the LigPrep module of the Schrödinger Maestro (Schrödinger Release, 2023-4; Schrödinger, LLC, New York, NY, https://www.schrodinger.com/life-sci ence/download/release-notes/release-2023-4). An OPLS4 force field was employed for energy minimization (Lu et al., 2021). LigPrep facilitates the conversion of 2D structures to three-dimensional structures by adding hydrogen atoms, adjusting bond lengths and angles, and selecting the conformer with the lowest conformational energy, which is influenced by the correct chiralities, tautomers, stereochemistry, and ring conformations. The default ionization state parameter employed was Epik, allowing for the generation of all possible protonation states, ionization states, tautomers, stereochemistry, and ring conformations. Stereoisomers were generated using the default parameters, with a maximum of 32 stereoisomers per ligand. Only the lowest-energy conformation was used for each ligand.

#### 2.2. Protein preparation and receptor grid generation

The three-dimensional structure of AR co-crystallized with DHT was obtained from the Protein Data Bank (PDB ID: 1T63) (https://www.rcsb. org) (Estébanez-Perpiñá et al., 2005). The PDB file of AR was processed using the Protein Preparation Wizard of Schrödinger Maestro. This tool removes water molecules, adds hydrogen atoms, fills missing loops, caps termini, adjusts charge states, and corrects inappropriate hydrogen bond assignments. Protein concentration was minimized using an OPLS4 force field. A Glide receptor grid generation module with default parameters, including van der Waals radius scaling factors (1.0) and a partial charge cutoff (0.25), was employed. Receptor grid generation refers to the computational definition of the protein's binding site, which provides the spatial and energetic parameters required for docking simulations. In this study, the grid was centered on the co-crystallized ligand DHT to ensure that docking was focused on the biologically relevant active site.

5α-Dihydrotestosterone (DHT) is a potent endogenous androgen derived from testosterone, known to bind the AR with high affinity. Upon binding, DHT induces AR dimerization, nuclear translocation, and transcriptional activation of AR-regulated genes. In this study, the cocrystallized DHT molecule served as a reference ligand for evaluating the binding affinity and structural interactions of synthetic compounds. The co-crystallized ligand DHT, situated in the binding site of AR, was considered during grid generation. Finally, a receptor grid was generated by selecting the centroid of the workspace ligands for molecular docking. These parameter values—the van der Waals radius scaling factor (1.0) and the partial charge cutoff (0.25)—are the default settings employed by Schrödinger's Glide receptor grid generation module, as specified in the Schrödinger Knowledge Base (Schrödinger, 2024). Using these defaults ensures consistent treatment of steric and electrostatic interactions, and supports methodological reproducibility in molecular docking studies.

#### 2.3. Molecular docking and binding energy calculations-MM/GBSA

Molecular docking of BPs, hydroxyflutamide, and flutamide with the co-crystallized ligand DHT with AR was performed using the Glide module of Schrödinger, employing the Standard Precision protocol with default parameters (Friesner et al., 2004). Additionally, MM/GBSA calculations were employed for precise binding energy determination utilizing the docked complexes obtained from Glide. The Schrödinger Prime-MM/GBSA module was utilized to calculate the binding energy ( $\Delta G$  bind) using the Volume Surface Generalized Born salvation model and OPLS4 force field.

# 2.4. DFT calculations

DFT calculations were used to predict the chemical reactivity of BPs, hydroxyflutamide, and flutamide in comparison with that of DHT. The aim of these calculations was to determine the HOMO and LUMO frontier molecular orbitals to provide a deeper understanding of the actions of BPs, flutamide, hydroxyflutamide, and DHT on AR. The DFT method, implemented in the Jaguar module of the Schrödinger Maestro, was employed to calculate the molecular orbitals using default parameters (Bochevarov et al., 2013).

# 2.5. MDS

To evaluate the structural and conformational stability of AR in complex with BPs, flutamide, and hydroxyflutamide, MDS were performed using Desmond. The AR-DHT complex was used as a reference model to represent the natural ligand-bound state of the receptor. Solvation was achieved with a TIP3P water model within an orthorhombic periodic boundary box (Jorgensen et al., 1983; Yazdani et al., 2023). The dimensions of the box were uniformly set to 10 Å along each axis, and the angles of the box were fixed at 90°. To maintain charge

neutrality, Cl<sup>-</sup> ions were added to the system. All other relevant parameters such as bond lengths and angles were retained at their default values. A system was built for AR and its docked complexes using an OPLS4 force field. Subsequently, the minimized model was employed for MDS for 500 ns. These simulations were performed within the NPT ensemble at a constant temperature of 300 K and a pressure of 1.01325 bar. The trajectories generated during the MDS were analyzed using the simulation interaction diagram module of Desmond to investigate the behavior and interactions of the selected compounds with AR.

# 2.6. Post-MDS MM/GBSA

Post-MDS binding energy calculations were performed using the MM/GBSA method. The Schrödinger Python script, thermal\_mmgbsa. py, was employed to evaluate the  $\Delta G$  bind for the AR-BPs, AR-hydroxyflutamide, and AR-flutamide. This script utilizes the MD trajectory generated by Desmond, dividing it into individual frame snapshots and subjecting each to MM/GBSA analysis. During the MM/GBSA calculation, 1000 snapshots from the 500 ns MDS were utilized to compute various types of energies, including van der Waals interactions, Coulomb energy, H-bonding contributions, lipophilic energy,  $\pi$ - $\pi$  packing energy, generalized Born electrostatic solvation energy, and total binding free energy ( $\Delta G$  bind) (Yazdani et al., 2023).

#### 2.7. Bret-based AR dimerization assay

A bioluminescence resonance energy transfer (BRET)-based assay was used to investigate the effects of the BPs on AR dimerization. The study was conducted following the protocol established by Pathak et al. (2024). The stably transfected HEK293 cells were obtained from routinely maintained in a 5 % CO2 atmosphere at 37 °C in MEM supplemented with 10 % FBS, 50 U/ml penicillin–streptomycin, 100  $\mu g/ml$ hygromycin B and 400  $\mu g/ml$  G418. For the NanoBRET-based AR dimerization assay, stably transfected HEK293 cells were seeded at a density of  $2.2 \times 10^5$  cells/ml in 90  $\mu$ l of assay medium (MEM medium supplement with 4 % charcoal-stripped FBS, 100 µg/ml hygromycin B and 400  $\mu$ g/ml G418) in a 96-well white cell culture microplate and were incubated for 1 h at 37 °C in a 5 % CO2 atmosphere. During incubation, the chemical assay was administered with 1  $\mu M$  HaloTag® NanoBRET  $^{\text{\tiny TM}}$  618 ligand (Promega, Cat. #. N1661) in a test environment according to the manufacturer's instructions. The cells were treated with 10 μl of the prepared chemicals and incubated at 37 °C in a 5 % CO<sub>2</sub> atmosphere for 24 h. Vehicle control (VC) and positive control (PC) wells contained 0.1 % DMSO and 10 nM DHT, respectively. In the BRETbased AR dimerization assay, the final concentration of DMSO in the assay medium was less than 0.13 % (v/v). Luminescence and fluorescence were measured 24 h after chemical treatment using the GloMax multimode plate reader (Promega, USA).

#### 2.8. ARE luciferase activity assay

To confirm the effects of ER $\alpha$ - and AR-mediated responses on BPs-induced hormone response element-dependent luciferase activities, the protocols for OECD test guideline No. 458 (OECD, 2023) were applied using the 22Rv1/MMTV\_GR-knockout cell lines (Korean Collection for Type Cultures, Jeongeup, Korea; KTCT No. HC30009). BP-mediated AR agonistic effects were determined using the 22Rv1/MMTV cell line expressing AR. The 22Rv1/MMTV\_GR-KO cells are maintained in culture medium (RPMI1640 supplemented with 10 % FBS (Invitrogen, CA, USA), 2 mM GlutaMAX (Invitrogen, CA, USA), 100 units/mL penicillin, 100 µg/mL streptomycin, and 0.25 µg/mL amphotericin B) that includes 200 µg/mL hygromycin (Invitrogen, CA, USA) as a luciferase gene selection marker to be used the first time after thawing cells. 0.1 % trypsin-EDTA is recommended for passage of 22Rv1/MMTV\_GR-KO cell line, because the higher concentration improves cell dissociation from the cell culture plate. For the assay, cells were suspended at

 $3.0 \times 10^5$  cells/mL in test medium (phenol red-free RPMI1640 supplemented with 10 % dextran-coated charcoal treated FBS (DCC-FBS; Invitrogen, CA, USA), 2 mM GlutaMAX, 100 units/mL penicillin, 100  $\mu g/mL$  streptomycin, and 0.25  $\mu g/mL$  amphotericin B). 100  $\mu L$  aliquots of the suspended cells (corresponding to  $3.0 \times 10^4$  cells/well) were transferred into a 96-well plate. Cells were pre-incubated for 48 h at 37  $^{\circ}\text{C}$  in a 5 % CO<sub>2</sub> incubator prior to chemical exposure. After incubation for 48 h, chemicals were serially diluted at a ratio of 1:10 in DMSO and then, the dilution are added to test medium to achieve a final DMSO concentration of 0.1 %. The medium from the assay plate was removed, replaced with the diluted chemical, and assay plates were incubated at 37 °C in a 5 % CO<sub>2</sub> incubator for 24 h. For the cell viability, CellTiter-Fluor™ assay reagent (Promega, WI, USA) of 20 µL, prepared according to manufacturer's instructions, was added into the assay wells. And the contents of the 96-well plate were briefly mixed on an orbital shaker and incubated for 2 h at 37  $^{\circ}\text{C}$ . The fluorescence was measured using a fluorometer (380-400 nm Ex/505 nm Em). For the luciferase activity, Steady-Glo® Luciferase assay reagent (Promega, WI, USA) of 50 µL, prepared according to manufacturer's instructions, was added directly into the assay wells after the cell viability assay. And the 96-well plate was blocked the light and left for 10 min. The luciferase activity was measured using a luminescence reader. For the agonist assay, reference standards (positive; DHT and mestanolone, negative; DEHP) were included, the response of AR agonistic positive control (10 nM DHT) should be at least 13.0, and the induction fold of PC<sub>10</sub> should be greater than 1+2 standard deviations (SD) of the induction of VC.

#### 2.9. Expression of BP-mediated whole AR proteins by western blot

Cell lysates were separated using 10 % SDS-PAGE and transferred to polyvinylidene difluoride membranes (Bio-Rad, Hercules, CA, USA). The membranes were blocked with 5 % skim milk in Tris-buffered saline containing 0.1 % Tween 20 (TBST) at room temperature for 1 h. The membranes were incubated with primary antibodies (androgen receptor, CST, Cat. No. 5153,  $\beta$ -actin, CST, Cat. No. 3700) in TBST at 4 °C overnight. The membranes were then incubated with the secondary antibody (Anti-mouse IgG, HRP-linked Antibody, CST, Cat. No. 7076) at room temperature for 1 h and washed with TBST. Finally, bands were detected using ECL reagents (SuperSignal  $^{\rm TM}$  West Pico PLUS Substrate, Thermo Fisher Scientific, Waltham, MA, USA).

# 2.10. Statistical analysis

All data were analyzed using Prism 8 (GraphPad Software Inc., San Diego, CA, USA), with  $p<0.05\ regarded$  as statistically significant. The interactions between activity and BPs were evaluated using one-way

analysis of variance. All values are presented as mean  $\pm$  standard deviation.

#### 3. Results

# 3.1. Molecular docking and molecular mechanics with generalized Born and surface area continuum solvation (MM/GBSA) quantification of the binding energies of BPs, hydroxyflutamide, and flutamide with AR

The interactions of selected compounds with the AR were evaluated using molecular docking. To better understand the binding behavior of BPs in comparison to known AR antagonists hydroxyflutamide and flutamide, we also assessed the binding free energy of the co-crystallized natural ligand DHT with AR. The docking score of the co-crystallized DHT was -12.582 kcal/mol. In general, lower docking scores indicate stronger predicted binding affinities between ligands and their targets. The predicted docking scores for BP-1, BP-2, BP-3, hydroxyflutamide, and flutamide were -8.025, -7.610, -7.229, -7.208, and -7.078 kcal/ mol, respectively (Table 1). To validate and refine the binding affinity, MM/GBSA binding free energy calculations were performed on the docked complexes. The predicted MM/GBSA binding free energies for DHT, BP-1, BP-2, BP-3, hydroxyflutamide, and flutamide were -85.29. -44.29, -45.04, -35.69, -48.28, and -41.28 kcal/mol, respectively. These results confirm that DHT has the strongest binding affinity for AR consistent with its role as the endogenous ligand. Among the tested compounds, BP-2 and hydroxyflutamide exhibited relatively higher binding affinities compared to the other ligands. The two-dimensional (2D) protein-ligand interaction diagram in Fig. 1 highlights key molecular interactions such as hydrogen bonds, hydrophobic contacts,  $\pi$ – $\pi$ stacking and other non-covalent interactions that contribute to ligand binding with AR.

#### 3.2. Density functional theory (DFT) calculations

The highest occupied molecular orbital (HOMO) and lowest unoccupied molecular orbital (LUMO) frontier molecular orbitals were analyzed using DFT, utilizing the Jaguar module of Schrödinger. This analysis offers insights into the energies associated with the occupied and unoccupied orbitals. Fig. 2 shows the frontier molecular orbitals of selected compounds with reference to DHT. The broader the energy gap within a molecule, indicates higher stability and lower reactivity. Conversely, a narrow energy gap correlates with decreased stability and increased reactivity because electron transitions occur more readily. As shown in Table 2 and Fig. 2, DHT had a higher energy gap (6.04 eV) than the other selected compounds, whereas hydroxyflutamide had a lower energy gap (4.46 eV). However, BPs and flutamide had similar energy

Table 1
Binding free energies (Kcal/mol) of DHT, Benzophenone derivatives, hydroxyflutamide, and flutamide with AR.

Compound	PubChem CID	Docking score	Glide GScore	Glide emodel	MM/ GBSA	Interacting amino acid residue
DHT	Reference ligand	-12.582	-12.582	-95.635	-85.29	Leu701, Leu704, <b>Asn705</b> , Leu707, Gly708, <b>Gln711</b> , Trp741, Met742, Met745, Val746, Met749, Arg752, Phe764, Met780, Met787, Leu873, Phe876, <b>Thr877</b> , Leu880, Phe891, Ile899
BP-1	CID: 8572	-8.025	-8.522	-57.947	-44.29	Leu701, Leu704, Asn705, Leu707, Gly708, Gln711, Trp741, Met745, Val746, Met749, Arg752, Phe764, Met780, Leu873, Thr877, Met895, Ile899
BP-2	CID: 8571	-7.610	-8.325	-63.045	-45.04	Leu701, Leu704, Asn705, Leu707, Gly708, Gln711, Trp741, Met745, Val746, Met749, Arg752, Phe764, Met780, Met787, Leu873, Thr877, Phe891, Met895, Ile899
BP-3	CID: 4632	-7.229	-7.392	-50.635	-35.69	Leu701, Leu704, Asn705, Leu707, Gly708, Gln711, Trp741, Met742, Met745, Val746, Met749, Arg752, Phe764, Met780, Leu873, Phe876, Thr877, Leu880, Phe891, Ile899, Met895
Hydroxyflutamide	CID: 91,649	-7.208	-7.209	-55.638	-48.28	Leu701, Leu704, Asn705, Leu707, Gly708, Gln711, Trp741, MET742, Me t745, Val746, Met749, Arg752, Phe764, Met787, Met780, Leu873, Phe876, Thr877, Met880, Phe891, Ile899
Flutamide	CID: 3397	-7.078	-7.078	-46.801	-41.28	Leu701, Leu704, Asn705, Leu707, Gly708, Gln711, MET742, Met745, Val746, Met749, Arg752, Phe764, Met780, Met787, Leu873, Phe876, Thr877, Leu880, Phe891

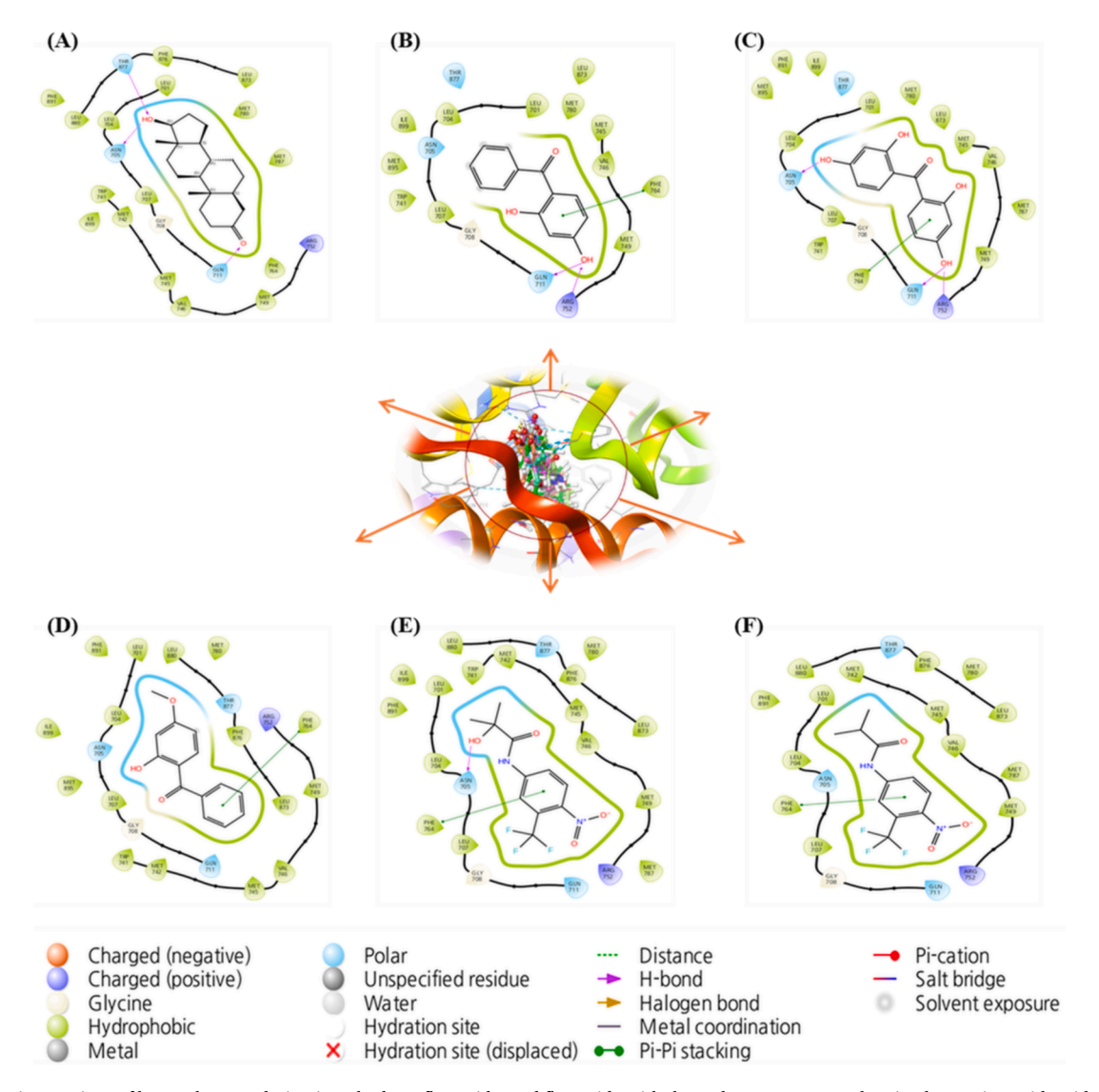


Fig. 1. Binding interactions of benzophenone derivatives, hydroxyflutamide, and flutamide with the androgen receptor, showing key amino acid residues involved in protein–ligand interactions. Panels represent (A) DHT, (B) BP-1, (C) BP-2, (D) BP-3, (E) Hydroxyflutamide, and (F) Flutamide. Interaction types are color-coded according to Schrodinger software's default settings.

gaps, and only slight differences were observed. The chemical reactivities of the BPs, hydroxyflutamide, and flutamide were high, allowing for rapid favorable interactions with AR.

# 3.3. MDS

MDS was employed to investigate the dynamic behavior of the AR in its unbound form and when bound to reference ligands DHT as well as BPs, flutamide, and hydroxyflutamide. Several key parameters were analyzed to understand the structural stability and dynamic characteristics of AR. To assess stability, the root mean square deviation (RMSD) of the trajectories over 500 ns was calculated. A lower RMSD indicates greater structural stability. All systems, including unbound AR and the docked complexes showed low RMSD values, suggesting stable conformations. The average RMSD for unbound AR was 1.65 Å. The RMSD values for AR-DHT, AR-BP-1, AR-BP-2, AR-BP-3, AR-hydroxyflutamide, and AR-flutamide were 1.53, 1.56, 1.64, 1.49, 1.86, and 1.49 Å, respectively (Fig. 3G). These values indicate that the structural deviations in AR-ligand complexes were comparable to that of the native AR-DHT complex. Notably, the AR-BP-2 and AR-hydroxyflutamide complexes, which demonstrated high binding affinity in docking studies, maintained equilibrium throughout the simulation. Overall, the

analysis suggests that all systems reached equilibrium and formed stable complexes (Supplementary Figs. 1–6). Furthermore, root mean square fluctuation (RMSF) analysis provided insights into the flexibility and mobility of individual amino acid residues. RMSF was evaluated for AR and its complexes over 500 ns. The average RMSF for unbound AR was 0.81 Å. For AR bound to DHT, BP-1, BP-2, BP-3, hydroxyflutamide, and flutamide, the RMSF values were 0.79, 0.79, 0.85, 0.77, 0.89, and 0.80 Å, respectively. Increased RMSF values observed in the AR-BP-2 and AR-hydroxyflutamide complexes suggest ligand-induced alterations in AR residue flexibility (Fig. 3H).

Additionally, the interactions between AR and selected ligands were monitored throughout the molecular dynamics simulation (Fig. 3A–F). These interactions were categorized into hydrogen bonds, hydrophobic interactions, ionic bonds, and water bridges. The predicted interaction profiles indicated that DHT, BP-2, and hydroxyflutamide formed a greater number of hydrogen bonds with AR compared to the other compounds. Furthermore, the timeline of protein–ligand contacts over the 500 ns simulation was analyzed using Schrödinger's Simulation Interaction Diagram module. This analysis revealed the frequency and nature of contacts between AR and each ligand, as well as the specific amino acid residues involved. The highest number of contacts (ranging from 0 to 9) was observed for AR-DHT, AR-BP-2, AR-hydroxyflutamide,

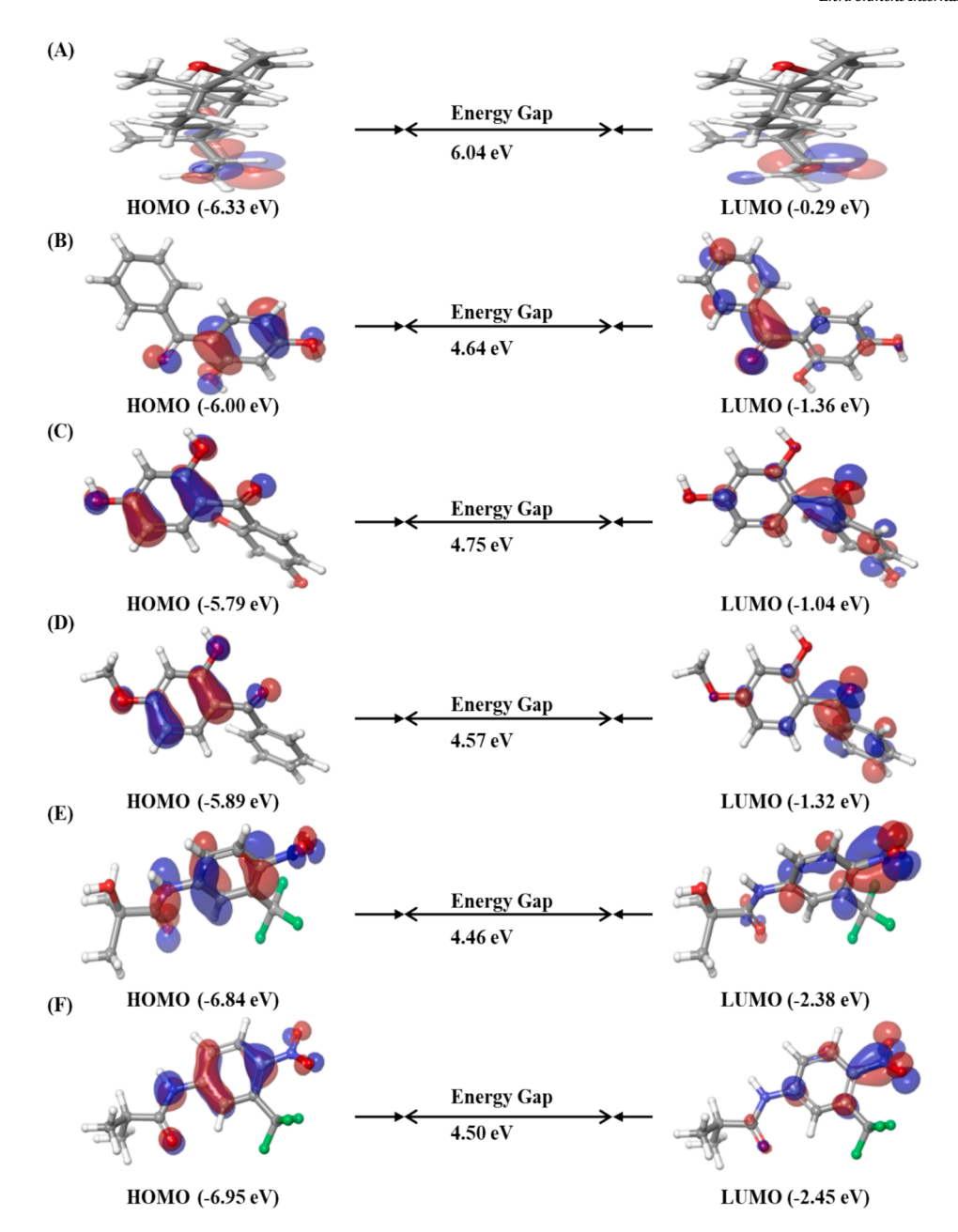


Fig. 2. Density Functional Theory (DFT) chemical reactivity analyses of the selected compounds. The figure depicts the frontier molecular orbitals HOMO (Highest Occupied Molecular Orbital) and LUMO (Lowest Unoccupied Molecular Orbital) for (A) DHT, (B) BP-1, (C) BP-2, (D) BP-3, (E) Hydroxyflutamide, and (F) Flutamide. The spatial distribution of the HOMO and LUMO orbitals provides insight into electron density and potential reactive sites of the compounds.

**Table 2**Comparisons of the energy levels of the Highest Occupied Molecular Orbital (HOMO), Lowest Unoccupied Molecular Orbital (LUMO), and the Energy Gap.

Substances	HOMO (eV)	LUMO (eV)	Energy Gap (eV)
DHT	-6.33	-0.29	6.04
BP-1	-6.00	-1.36	4.64
BP-2	-5.79	-1.04	4.75
BP-3	-5.89	-1.32	4.57
Hydroxyflutamide	-6.84	-2.38	4.46
Flutamide	-6.95	-2.45	4.50

and AR-flutamide, while the remaining complexes showed fewer contacts (0–6). Detailed contact analyses for AR-BP-2 and AR-hydroxyflutamide, including the interacting residues, are presented in Figs. S3 and S5, respectively. An assessment of the interaction strength

throughout the simulation revealed that BP-2 and hydroxyflutamide maintained more consistent and stronger contacts with AR (SI Appendix). Specifically, BP-2 showed contact persistence with AR residues Gln711, Phe764, and Asn705 for 43 %, 75 %, and 99 % of the simulation time, respectively (Fig. S3). Similarly, hydroxyflutamide maintained strong interactions with Leu704, Asn705, Phe764, and Thr877 for 38 %, 65 %, 35 %, and 33 % of the simulation time, respectively (Fig. S5).

# 3.4. Post-MDS binding energy calculations using MM/GBSA

To support and validate the results of molecular docking and MDS, post-MDS binding free energy ( $\Delta Gbind$ ) calculations were carried out using the MM/GBSA method. This approach offers a more realistic and dynamic estimate of binding affinity utilizing trajectories data obtained from MDS. The calculated  $\Delta Gbind$  values and other energy components are summarized in Table 3. As expected, DHT, the natural ligand of the

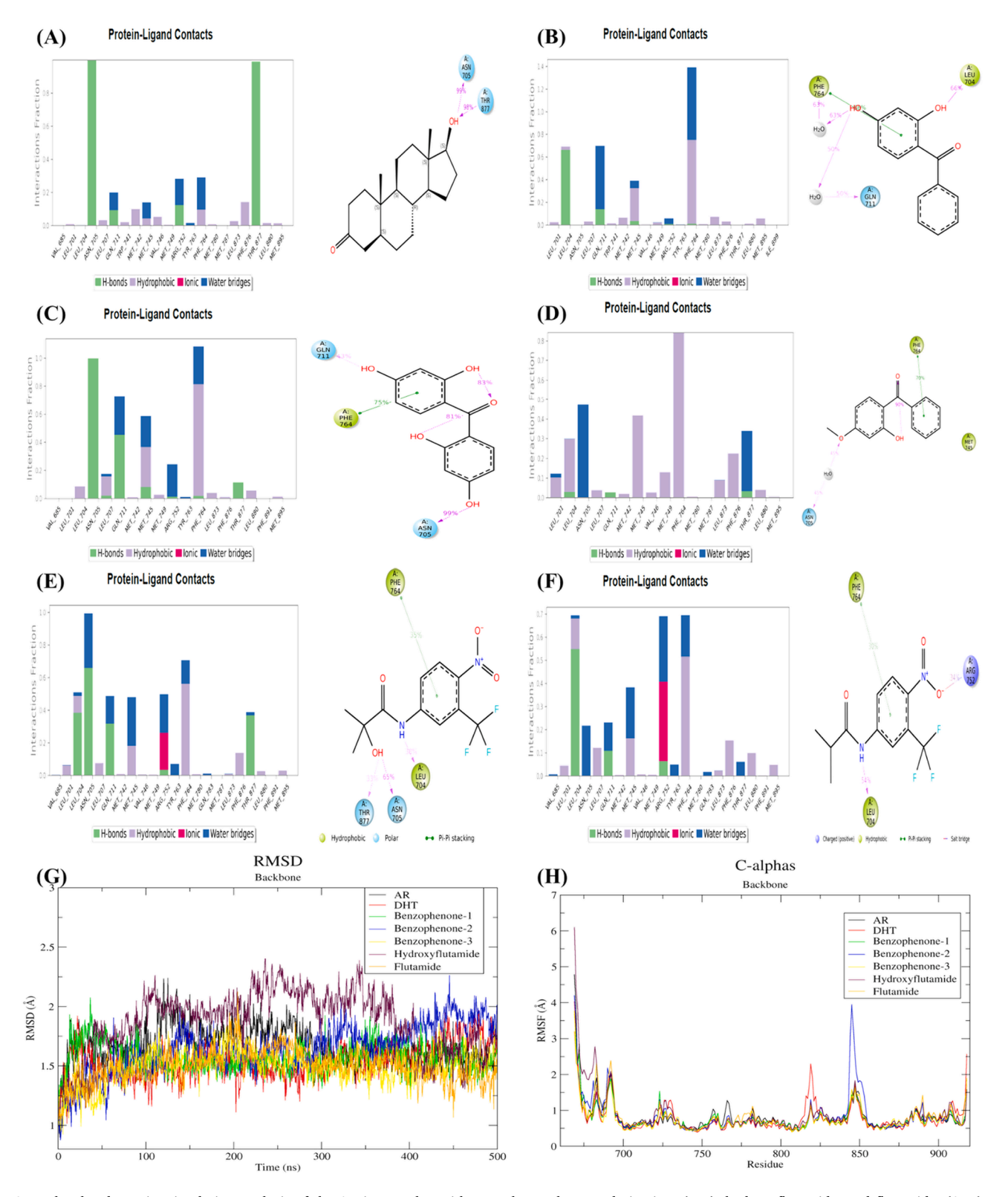


**Fig. 3.** Molecular dynamics simulation analysis of the AR in complex with DHT, benzophenone derivatives (BPs), hydroxyflutamide, and flutamide. (A–D) Protein–ligand interaction profiles including timeline contacts over 500 ns and interaction types that occurred in more than 30 % of the simulation time. (A) AR-DHT, (B) AR-BP-1, (C) AR-BP-2, (D) AR-BP-3, (E) AR-hydroxyflutamide, and (F) AR-flutamide. (G) Root mean square deviation (RMSD) plot showing the structural stability of AR and its ligand-bound complexes. (H) Root mean square fluctuation (RMSF) analysis depicting residue-wise flexibility of AR in the presence of different ligands.

Table 3

Average predicted binding free energies (kcal/mol) obtained via post-molecular dynamics simulation MM/GBSA calculations.

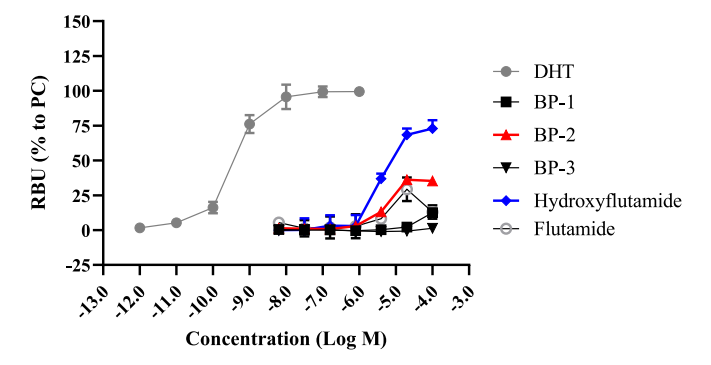
	DHT_CID_10635	BP-1	BP-2	BP-3	Hydroxyflutamide	Flutamide
$\Delta G_{vdw}$	-48.11	-38.42	-38.41	-41.50	-41.47	-41.69
$\Delta G_{coul}$	-21.16	-8.48	-29.81	-0.95	-19.81	-14.28
$\Delta G_{Hbond}$	-0.70	-0.11	-0.19	-0.06	-0.23	-0.16
$\Delta G_{\text{Lipo}}$	-27.24	-16.11	-10.22	-20.15	-16.25	-16.36
$\Delta G_{Pack}$	0	-0.98	-0.83	-0.93	-0.74	-0.70
$\Delta G_{SolGB}$	20.91	17.86	31.27	10.85	22.20	21.22
$\Delta G_{bind}$	-75.29	-44.97	-46.39	-52.07	-54.93	-50.96

 $\Delta G_{vdw}$ : Contribution of van der Waals interaction energy to binding free energy;  $\Delta G_{coul}$ : Contribution of Coulomb energy to binding free energy;  $\Delta G_{Hbond}$ : H-bonding contributions to binding free energy;  $\Delta G_{Pack}$ :  $\pi$ - $\pi$  packing energy contribution to binding free energy;  $\Delta G_{SolGB}$ : Generalized Born electrostatic solvation energy contribution to binding free energy.  $\Delta G_{bind}$ : Total binding free energy.

AR showed the strongest binding affinity (-75.29 kcal/mol). Among the benzophenone derivatives, BP-2 displayed a more favorable binding energy (-46.39 kcal/mol) compared to BP-1 (-44.97 kcal/mol) and BP-3 (-52.07 kcal/mol). BP-2 also had the most favorable hydrogen bond energy (-0.19 kcal/mol), suggesting stronger and more stable interactions with AR. Similarly, hydroxyflutamide showed a higher binding affinity (-54.93 kcal/mol) than flutamide (-50.96 kcal/mol). Taken together, these MM/GBSA results are consistent with the docking and MDS analyses, highlighting BP-2 and hydroxyflutamide as the most stable and energetically favorable AR binders among the compounds studied.

#### 3.5. Findings from cell-based assays on BPs in laboratory models

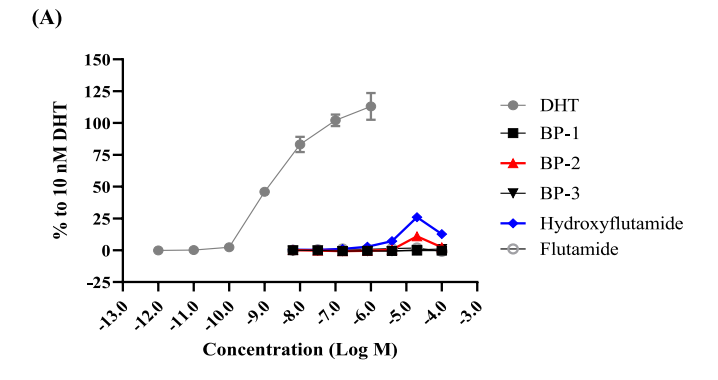
Previously, the binding affinities of BP and its derivatives were measured using a computational approach. Here, a cell-based assay was performed to compare the results. Fig. 4 confirms the dimerization activity of cytoplasmic AR through BRET assay in vitro. Compared to the positive control group (with DHT concentrations ranging from -6.0 to  $-10.0 \log M$ ), the cytoplasmic AR dimerization was relatively weak for BPs. Among the BP derivatives, AR dimerization was highest with BP-2 treatment, which increased at three concentrations (-4.0, -4.7, and −5.4 log M). BP-1 showed dimerization only at the highest concentration (-4.0 log M). BP-3 did not demonstrate any dimerization with AR. The results for BP-2 closely paralleled those of the compound, hydroxyflutamide, in terms of data trends. For hydroxyflutamide, dimerization also increased at -4.0, -4.7, and -5.4 log M. As shown in Fig. 4, BP-2 induced a moderate but concentration-dependent increase in AR dimerization activity, reaching approximately 35 % of the DHT response at its highest effective concentration (-4.0 log M). This trend was similar to that of hydroxyflutamide, which showed a stronger maximal response (~73 %) under comparable conditions. In contrast, BP-1 exhibited weak activity only at the highest concentration, and BP-3 showed no measurable dimerization. These results suggest that BP-2 acts as a partial AR agonist, consistent with previous computational



**Fig. 4.** Dose-response curves of bioluminescence resonance energy transfer signals.

predictions of its relatively high binding affinity.

Based on the BRET assay results, agonistic and antagonistic assays were performed. The results of the AR agonistic assay (Fig. 5A) revealed the same trend as that of the BRET assay. The PC10 values for BP-2 and its reference compound hydroxyflutamide, were  $1.75 \times 10^{-5}$  and 1.41 $\times$  10<sup>-8</sup> M, respectively. Fig. 5B displays the antagonistic activity for BP-1, BP-2, BP-3, and the reference compounds hydroxyflutamide and flutamide. The IC<sub>30</sub> and IC<sub>50</sub> values for the BPs were  $2.77 \times 10^{-7}$  and 9.47 $\times$   $10^{-7}$  M for BP-1,  $1.67\times10^{-7}$  and  $3.10\times10^{-7}$  M for BP-2, and  $5.70\times$  $10^{-7}$  and  $1.45 \times 10^{-6}$  M for BP-3. Bicalutamide was used as a positive control. Because of the cytotoxicity exhibited by the BPs at the highest concentrations, the data for those concentrations were omitted. In line with the BRET assay results, where BP-2 exhibited approximately 35 % dimerization activity relative to DHT, the AR transcriptional agonist assay also revealed a weak yet distinct response for BP-2. At  $-4.7 \log M$ , BP-2 induced 10.9 % of AR-mediated transcriptional activity compared to DHT, while other BPs showed no measurable activation. In the AR transcriptional antagonist assay, BP-2 and hydroxyflutamide produced similar inhibition profiles, with 81.3% and 75.8% inhibition at  $-4.7\log$ M, respectively. These values were lower than those of BP-1, BP-3, and



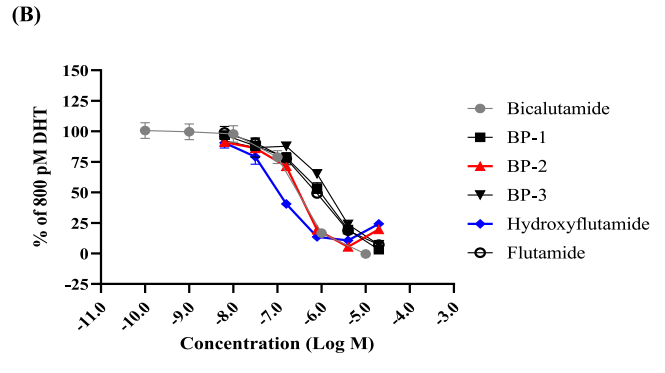


**Fig. 5.** Dose-response curves from AR agonistic test (A) and AR antagonistic test (B) in reporter gene assay using 22Rv1/MMTV\_GRKO cell line (OECD TG No.458).

flutamide, which exceeded 90 %. These results suggest that BP-2 exhibits partial agonist and antagonist characteristics and shares structural features with hydroxyflutamide, as supported by computational predictions. The consistency among the BRET, luciferase assays, and docking results reinforces the mechanistic plausibility of BP-2's ARbinding behavior.

#### 3.6. Induction of whole AR protein expression by BPs

The binding affinity of the cytoplasmic AR to BP-1, BP-2, and BP-3 was evaluated using various assays. The results consistently showed changes in the AR protein expression in response to these compounds. In the case of BP-2, a significant positive response was produced at -4.7 log M in the agonistic assay, closely mirroring the quantitative pattern observed in the positive control group treated with DHT (Fig. 6). In the antagonistic assay, the lowest active concentration of BP-2 was  $-5.4 \log$ M, leading to a decrease in AR expression compared to the vehicle control, and resulting in a U-shaped response curve. Both BP-1 and BP-3 exhibited comparable patterns, consistent with the findings of the cellular assays (Fig. 6). As shown in Fig. 6, BP-2 induced a marked increase in AR protein expression at -4.7 log M, reaching levels comparable to those of DHT-treated cells. At −5.4 log M, however, BP-2 significantly decreased AR expression, forming a U-shaped response curve. The statistical grouping in Fig. 6B shows that BP-2 at -5.4 log M ('e') differed significantly from DHT ('a') and from BP-2 at -4.7 log M ('ab'), confirming a concentration-dependent modulation of AR levels. BP-1 and BP-3 showed similar, though less pronounced, patterns. These protein-level results are consistent with the functional trends observed in BRET and reporter assays and are further supported by computational docking predictions. The computational analysis results corresponded with experimental data, highlighting similarities in structure and binding between the BP compounds and DHT (a positive control in AR dimerization and transcription assays), as well as with hydroxyflutamide, a partial agonist/antagonist. This suggests that similar computational approaches could be useful for predicting the potential of untested chemicals with structural and binding profiles comparable to those of known endocrine disruptors.

#### 4. Discussion

Molecular docking analyses confirmed that DHT has the strongest binding affinity for AR, consistent with its well-documented role in ARmediated signaling pathways (Chatterjee, 2003; Roy et al., 1999). However, synthetic compounds, such as BP-1, BP-2, and BP-3, which are part of the BP family, have recently gained attention because of their potential as endocrine disruptors. As commonly used UV filters, these compounds exhibit varying degrees of affinity for AR. Among them, BP-2 demonstrated the strongest interaction with AR, as indicated by its superior docking scores and binding energies compared with those of BP-1 and BP-3. BP derivatives are recognized as EDCs capable of interfering with the function of steroid receptors, including AR (Schreurs et al., 2002). MM/GBSA calculations, which highlight the significant hydrophobic and hydrogen bond interactions of BP-2 with key AR residues such as Gln711 and Asn705, explains its enhanced binding affinity (Coffey and Robson, 2012). Although BP-2 showed the strongest binding, BP-1 and BP-3 also displayed notable affinities, suggesting their potential as AR-mediated endocrine disruptors.

DFT calculations provided additional insights into the chemical profiles of BP-1, BP-2, and BP-3. BP-2 exhibited a well-balanced HOMO–LUMO energy gap, indicating an optimal combination of stability and reactivity, making it particularly suitable for AR interactions. In comparison, BP-1 and BP-3 had slightly lower energy gaps, implying higher reactivity but reduced stability over time. Hydroxyflutamide showed the smallest energy gap as a reference, highlighting its increased reactivity (Olugbogi et al., 2024; Xie et al., 2022). These molecular predictions align with the laboratory findings, where the stable chemical profile of BP-2 was associated with more consistent antagonistic effects on AR, whereas BP-1 and BP-3 showed greater variability.

RMSD and RMSF analyses revealed that all three BPs induced conformational changes in AR, which contributed to their antagonistic effects. BP-2 induced minimal structural deviations, resulting in a more stable AR-ligand complex, whereas BP-1 and BP-3 introduced greater flexibility. These conformational changes are crucial for understanding how each compound modulates the AR activity. Khan et al. (2022) reported that ligand-induced conformational shifts are key for altering receptor activity, supporting the predictions made by molecular simulations. Laboratory assays confirmed that the ability of BP-2 to induce

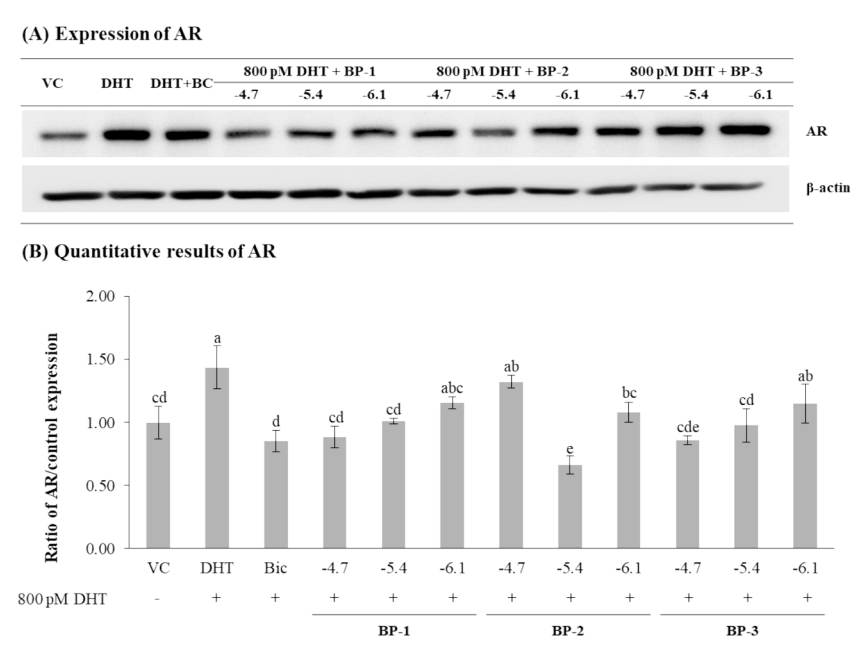


**Fig. 6.** AR proteins (A) expression and (B) quantitative results induced by DHT in the presence and the absence of AR antagonist bicalutamide (Bic) and BPs. Alphabetical labels (a–e) in panel B indicate statistically significant groupings of each treatment group. Groups sharing the same letter are not significantly different from each other, whereas groups with no shared letters are significantly different (p < 0.05).

stable conformational changes resulted in stronger and more sustained antagonistic effects, whereas BP-1 and BP-3 produced more transient effects, consistent with their predicted behavior.

Molecular simulations underscored the importance of hydrogen bonding and hydrophobic interactions in the stabilization of AR-ligand complexes. BP-2 formed the most robust interactions with key AR residues, such as Gln711, Phe764, and Asn705, compared to BP-1 and BP-3. These interactions are essential for stabilizing the AR-ligand complex and modulating receptor function. Xie et al. (2022) and Brown et al. (2023) emphasized that the orientation and functional groups of ligands play a crucial role in optimizing hydrogen bonding for AR modulation. Laboratory models confirmed that the strong hydrogen bonding of BP-2 led to its greater antagonistic potency, whereas BP-1 and BP-3, although effective, exhibited weaker interactions.

Structurally, we propose that hydroxylation of parent compound induces enhancing the AR-mediated endocrine disrupting potential, and cell-based assays further validate our hypothesis. Regarding the AR antagonistic effect, the quantitative level of suppressing the AR-induced luciferase activity by flutamide was increased around 6.92-folds with IC<sub>50</sub> value after hydroxylation (hydroxyflutamide). Additionally, from the results of BRET assay in references, hydroxyflutamide induced the homodimerization of cytosolic ARs, whereas flutamide had no inducing effect on the homodimerization of cytosolic ARs. This homodimerization of cytosolic ARs by hydroxyflutamide developed the AR agonistic effect at specific concentration. These changing the AR-mediated endocrine disrupting potential depend on hydroxylation of parent chemical also exhibited in BPs. In the AR antagonist test, the quantitative level of suppressing the AR-induced luciferase activity induced by BP-1 was enhanced around 3.06-folds with IC50 value via hydroxylation of each phenol rings (BP-2). In terms of AR agonistic effect, homodimerization of ARs in cytosol by BP-2 linkages enhancing luciferase activity at specific concentration in AR agonist test, whereas BP-1 and BP-3 had no AR agonistic effects. This development of the AR agonistic effect of BP-2 seems to be due to translocation of cytosolic ARs to nucleus after dimerization by BP-2, because when ligands bind to the nuclear receptors within cells, the ligand-AR complex undergoes a conformational change in cytosol that leads to receptor activation and a transcriptional response (Park et al., 2021). Also, various publications highlighted that BP derivatives can modulate AR activity in a concentration-dependent manner, further supporting computational predictions (Brown et al., 2023; Azhagiya Singam et al., 2019; Liu et al., 2018; Sakkiah et al., 2018). In case of AR-mediated endocrine disrupting effect induced by polybrominated diphenyl ethers, their hydroxylated metabolites had stronger AR antagonistic effects than parent chemical in transactivation in vitro assay (Kojima et al., 2009). Similar observations have been reported with other compounds, suggesting hydroxylation can enhance AR-related activity regardless of functional direction. Moilanen et al. (2015) found that ORM-15341, a hydroxylated metabolite of darolutamide (ODM-201), exhibited greater binding affinity for AR and maintained potent antagonistic effects. Notably, hydroxylation has also been linked to the acquisition of agonist properties. For instance, Ariazi et al. (2007) showed that 17-hydroexemestane, a hydroxylated metabolite of exemestane, acted as an AR agonist and stimulated proliferation in T47D breast cancer cells. In a separate study, hydroxyflutamide induced partial AR activation at micromolar concentrations in HepG2 cells, whereas flutamide alone did not (Maness et al., 1998). These findings indicate that hydroxylation can amplify both agonistic and antagonistic activities of AR ligands, depending on concentration and cellular environment. With respect to association with docking amino acid residue and AR agonistic/antagonistic activities, Azhagiya Singam et al. (2019) pointed out that AR agonist/antagonist form has a hydrogen bond with Asn705 and that this interaction is absent for AR antagonist. BP-2 had an AR agonistic effect alongside AR antagonistic effect, consistent with a hydrogen bond with Asn705 in this study as well. These findings indicate that BP-2 is the most potent AR-mediated endocrine disruptor, with BP-1 and BP-3 exhibiting substantial

activities.

Combined insights from molecular docking, MM/GBSA calculations, DFT analysis, MDS, and cell-based assays indicate that BP-1, BP-2, and BP-3 are effective AR-mediated endocrine disruptors, with BP-2 demonstrating the greatest efficacy. The structural flexibility, strong hydrogen bonding, and balanced chemical properties of BP-2 contribute to its superior AR modulation. BP-1 and BP-3, although less stable, displayed notable antagonistic activities. The alignment between the molecular predictions and experimental validation highlights the potential of these compounds as AR-targeting agents and endocrine disruptors. Further research should focus on assessing the long-term toxicological effects of these compounds to fully understand their endocrine-disrupting potential.

#### 5. Conclusion

This study clarifies the mode of mechanism of endocrine-disrupting impacts of BPs, which are commonly found in cosmetics and environmental pollutants, via interaction with AR. Through the integration of molecular docking, molecular dynamics simulations and experimental validation, BP-2 was identified as potent agonist/antagonist of the AR, exhibiting binding affinities and structural interactions consistent with those of natural and established AR ligands. These results offer an enhanced comprehension of the impact of BP-2 and similar substances, which are synthesized by hydroxylation from parent compound, on AR activity, providing key insights into the structural components necessary for endocrine disruption.

#### CRediT authorship contribution statement

**Da-Hyun Jeong:** Writing – original draft, Investigation. **Rajesh Kumar Pathak:** Writing – original draft, Validation. **Da-Woon Jung:** Writing – review & editing, Conceptualization. **Jun-Mo Kim:** Data curation, Conceptualization. **Hee-Seok Lee:** Writing – review & editing, Writing – original draft, Validation, Project administration, Investigation, Funding acquisition, Data curation, Conceptualization.

# **Declaration of competing interest**

The authors declare that they have no known competing financial interests or personal relationships that could have appeared to influence the work reported in this paper.

# Acknowledgments

This research was supported by grants from the National Research Foundation of Korea grant (NRF-RS-2024-00345893) and the Ministry of Food and Drug Safety (21153MFDS605). This research was also supported by the Chung-Ang University Graduate Research Scholarship (Academic Scholarship for College of Biotechnology and Natural Resources) in 2021.

# Appendix A. Supplementary data

Supplementary data to this article can be found online at https://doi.org/10.1016/j.envint.2025.109632.

#### Data availability

No data was used for the research described in the article.

#### References

Alonso-Magdalena, P., Vieira, E., Soriano, S., Menes, L., Burks, D., Quesada, I., Nadal, A., 2010. Bisphenol a exposure during pregnancy disrupts glucose homeostasis in mothers and adult male offspring. Environ. Health Perspect. 118 (9), 1243–1250. https://doi.org/10.1289/ehp.1001993.

- Amano, I., Takatsuru, Y., Khairinisa, M.A., Kokubo, M., Haijima, A., Koibuchi, N., 2018. Effects of mild perinatal hypothyroidism on cognitive function of adult male offspring. Endocrinology 159 (4), 1910–1921. https://doi.org/10.1210/en.2017-03125
- Ariazi, E.A., Leitão, A., Oprea, T.I., Chen, B., Louis, T., Bertucci, A.M., Sharma, C.G.N., Gill, S.D., Kim, H.R., Shupp, H.A., Pyle, J.R., Madrack, A., Donato, A.L., Cheng, D., Paige, J.R., Jordan, V.C., 2007. Exemestane's 17-hydroxylated metabolite exerts biological effects as an androgen. Mol. Cancer Ther. 6, 2817–2827. https://doi.org/10.1158/1535-7163.MCT-07-0312.
- Axelstad, M., Hass, U., Scholze, M., Christiansen, S., Kortenkamp, A., Boberg, J., 2018.
  EDC IMPACT: Reduced sperm counts in rats exposed to human relevant mixtures of endocrine disrupters. Endocr. Connect. 7 (1), 139–148. https://doi.org/10.1530/EC-17.0307
- Azhagiya Singam, E.R., Tachachartvanich, P., La Merrill, M.A., Smith, M.T., Durkin, K.A., 2019. Structural dynamics of agonist and antagonist binding to the androgen receptor. J. Phys. Chem. B 123 (36), 7657–7666. https://doi.org/10.1021/acs.ipch/9b05654
- Bochevarov, A.D., Harder, E.D., Hughes, T., Greenwood, J.R., Braden, D.A., Philipp, D. M., Rinaldo, D., Halls, M.D., Zhang, J., Friesner, R.A., 2013. Jaguar: a high-performance quantum chemistry software program with strengths in life and materials sciences. Int. J. Quant. Chem 113 (18), 2110–2142. https://doi.org/10.1002//QUA.24481.
- Bohl, C.E., Wu, Z., Miller, D.D., Bell, C.E., Dalton, J.T., 2007. Crystal structure of the T877A human androgen receptor ligand-binding domain complexed to cyproterone acetate provides insight for ligand-induced conformational changes and structurebased drug design. J. Biol. Chem. 282 (18), 13648–13655. https://doi.org/10.1074/ ibc.M611711200.
- Brown, E.C., Hallinger, D.R., Simmons, S.O., 2023. High-throughput AR dimerization assay identifies androgen disrupting chemicals and metabolites. Front. Toxicol. 5, 1134783. https://doi.org/10.3389/ftox.2023.1134783.
- Cano-Sancho, G., Salmon, A.G., La Merrill, M.A., 2017. Association between exposure to *p,p*'-DDT and its metabolite *p,p*'-DDE with obesity: integrated systematic review and meta-analysis. Environ. Health Perspect. 125 (9), 096002. https://doi.org/10.1289/EHP527.
- Chatterjee, B., 2003. The role of the androgen receptor in the development of prostatic hyperplasia and prostate cancer. Mol. Cell. Biochem. 253 (1–2), 89–101. https://doi.org/10.1023/a:1026057402945.
- Coffey, K., Robson, C.N., 2012. Regulation of the androgen receptor by post-translational modifications. J. Endocrinol. 215 (2), 221–237. https://doi.org/10.1530/JOE-12-0238.
- Davey, R.A., Grossmann, M., 2016. Androgen receptor structure, function and biology: from bench to bedside. Clin. Biochem. Rev. 37 (1), 3–15.
- Dayan Elshan, N.G.R., Rettig, M.B., Jung, M.E., 2019. Molecules targeting the androgen receptor (AR) signaling axis beyond the AR-Ligand binding domain. Med. Res. Rev. 39 (3), 910–960. https://doi.org/10.1002/med.21548.
- Du, Y., Wang, W.Q., Pei, Z.T., Ahmad, F., Xu, R.R., Zhang, Y.M., Sun, L.W., 2017. Acute toxicity and ecological risk assessment of benzophenone-3 (BP-3) and benzophenone-4 (BP-4) in ultraviolet (UV)-filters. Int. J. Environ. Res. Public Health 14 (11), 1414. https://doi.org/10.3390/ijerph14111414.
- Estébanez-Perpiñá, E., Moore, J.M., Mar, E., Delgado-Rodrigues, E., Nguyen, P., Baxter, J.D., Buehrer, B.M., Webb, P., Fletterick, R.J., Guy, R.K., 2005. The molecular mechanisms of coactivator utilization in ligand-dependent transactivation by the androgen receptor. J. Biol. Chem. 280 (9), 8060–8068. https://doi.org/10.1074/jbc.M407046200.
- Freires, I.A., Sardi, J.C., de Castro, R.D., Rosalen, P.L., 2017. Alternative animal and nonanimal models for drug discovery and development: bonus or burden? Pharm. Res. 34 (4), 681–686. https://doi.org/10.1007/s11095-016-2069-z.
- 34 (4), 681–686. https://doi.org/10.1007/s11095-016-2069-z.
  Friesner, R.A., Banks, J.L., Murphy, R.B., Halgren, T.A., Klicic, J.J., Mainz, D.T., Repasky, M.P., Knoll, E.H., Shelley, M., Perry, J.K., Shaw, D.E., Francis, P., Shenkin, P.S., 2004. Glide: a new approach for rapid, accurate docking and scoring. 1. Method and assessment of docking accuracy. J. Med. Chem. 47 (7), 1739–1749. https://doi.org/10.1021/im0306430.
- Galli, C.M., 2014. El viento del sur de Aparecida a Río: El proyecto misionero latinoamericano en la teología y el estilo pastoral de Francisco. Seminarios. Sobre. Los. Ministerios. En. La. Iglesia. 60 (211), 9–48. https://doi.org/10.52039/ seminarios.v60i211.210.
- Gao, W., Bohl, C.E., Dalton, J.T., 2005. Chemistry and structural biology of androgen receptor. Chem. Rev. 105 (9), 3352–3370. https://doi.org/10.1021/cr020456u.
- Gelmann, E.P., 2002. Molecular biology of the androgen receptor. J. Clin. Oncol. 20 (13), 3001–3015. https://doi.org/10.1200/JCO.2002.10.018.
- Ghassabian, A., Trasande, L., 2018. Disruption in thyroid signaling pathway: a mechanism for the effect of endocrine-disrupting chemicals on child neurodevelopment. Front. Endocrinol. (Lausanne) 9, 204. https://doi.org/10.3389/ fendo.2018.00204.
- Giulivo, M., Lopez de Alda, M., Capri, E., Barceló, D., 2016. Human exposure to endocrine disrupting compounds: their role in reproductive systems, metabolic syndrome and breast cancer. A review. Environ. Res. 151, 251–264. https://doi.org/ 10.1016/j.envres.2016.07.011.
- Heindel, J.J., Skalla, L.A., Joubert, B.R., Dilworth, C.H., Gray, K.A., 2017. Review of developmental origins of health and disease publications in environmental epidemiology. Reprod. Toxicol. 68, 34–48. https://doi.org/10.1016/j. reprotox.2016.11.011.
- Heinlein, C.A., Chang, C., 2004. Androgen receptor in prostate cancer. Endocr. Rev. 25 (2), 276–308.
- Heurung, A.R., Raju, S.I., Warshaw, E.M., 2014. Benzophenones. Dermatitis 25 (1), 3–10. https://doi.org/10.1097/DER.000000000000025.

- Hollingsworth, S.A., Dror, R.O., 2018. Molecular dynamics simulation for all. Neuron 99 (6), 1129–1143. https://doi.org/10.1016/j.neuron.2018.08.011.
- Hong, H., Tong, W., Fang, H., Shi, L., Xie, Q., Wu, J., Perkins, R., Walker, J.D., Branham, W., Sheehan, D.M., 2002. Prediction of estrogen receptor binding for 58,000 chemicals using an integrated system of a tree-based model with structural alerts. Environ. Health Perspect. 110 (1), 29–36. https://doi.org/10.1289/ ebp.0211029
- Hospital, A., Goñi, J.R., Orozco, M., Gelpí, J.L., 2015. Molecular dynamics simulations: advances and applications. Adv. Appl. Bioinform. Chem. 8, 37–47. https://doi.org/ 10.2147/AABC.\$70333.
- Jefferson, W.N., Kinyamu, H.K., Wang, T., Miranda, A.X., Padilla-Banks, E., Suen, A.A., Williams, C.J., 2018. Widespread enhancer activation via ERα mediates estrogen response in vivo during uterine development. Nucl. Acids Res. 46 (11), 5487–5503. https://doi.org/10.1093/nar/gky260.
- Jin, Y., Duan, M., Wang, X., Kong, X., Zhou, W., Sun, H., Liu, H., Li, D., Yu, H., Li, Y., Hou, T., 2019. Communication between the ligand-binding pocket and the activation function-2 domain of androgen receptor revealed by molecular dynamics simulations. J. Chem. Inf. Model. 59 (2), 842–857. https://doi.org/10.1021/acs. icim.8b00796.
- Johansson, H.K.L., Svingen, T., Fowler, P.A., Vinggaard, A.M., Boberg, J., 2017. Environmental influences on ovarian dysgenesis – developmental windows sensitive to chemical exposures. Nat. Rev. Endocrinol. 13 (7), 400–414. https://doi.org/ 10.1038/nrendo.2017.36.
- Jorgensen, W.L., Chandrasekhar, J., Madura, J.D., Impey, R.D., Klein, M.L., 1983.
  Comparison of simple potential functions for simulating liquid water. J. Chem. Phys. 79, 926–935. https://doi.org/10.1063/1.445869.
- Kawamura, Y., Ogawa, Y., Nishimura, T., Kikuchi, Y., Nishikawa, J., Nishihara, T., Tanamoto, K., 2003. Estrogenic activities of UV stabilizers used in food contact plastics and benzophenone derivatives tested by the yeast two-hybrid assay. J. Health Sci. 49 (3), 205–212. https://doi.org/10.1248/JHS.49.205.
- Khan, S.H., Braet, S.M., Koehler, S.J., Elacqua, E., Anand, G.S., Okafor, C.D., 2022. Ligand-induced shifts in conformational ensembles that describe transcriptional activation. eLife 11, e80140. https://doi.org/10.7554/eLife.80140.
- Kojima, H., Takeuchi, S., Uramaru, N., Sugihara, K., Yoshida, T., Kitamura, S., 2009. Nuclear hormone receptor activity of polybrominated diphenyl ethers and their hydroxylated and methoxylated metabolites in transactivation assays using chinese hamster ovary cells. Environ. Health Perspect. 117, 1210–1218. https://doi.org/ 10.1289/ehp.0900753.
- La Merrill, M.A., Vandenberg, L.N., Smith, M.T., Goodson, W., Browne, P., Patisaul, H.B., Guyton, K.Z., Kortenkamp, A., Cogliano, V.J., Woodruff, T.J., Rieswijk, L., Sone, H., Korach, K.S., Gore, A.C., Zeise, L., Zoeller, R.T., 2020. Consensus on the key characteristics of endocrine–disrupting chemicals as a basis for hazard identification. Nat. Rev. Endocrinol. 16 (1), 45–57. https://doi.org/10.1038/s41574-019-0273-8.
- Lambright, C., Ostby, J., Bobseine, K., Wilson, V., Hotchkiss, A.K., Mann, P.C., Gray Jr., L.E., 2000. Cellular and molecular mechanisms of action of linuron: an antiandrogenic herbicide that produces reproductive malformations in male rats. Toxicol. Sci. 56 (2), 389–399. https://doi.org/10.1093/toxsci/56.2.389.
- Larry Jameson, J., De Groot, L.J., 2016. Endocrinology: Adult & Pediatric in Medicine, seventh ed. eBook. ISBN: 9780323321952.
- Liu, N., Zhou, W., Guo, Y., Wang, J., Fu, W., Sun, H., Li, D., Duan, M., Hou, T., 2018. Molecular dynamics simulations revealed the regulation of ligands to the interactions between androgen receptor and its coactivator. J. Chem. Inf. Model. 58 (8), 1652–1661. https://doi.org/10.1021/acs.jcim.8b00283.
- Lonergan, P.E., Tindall, D.J., 2011. Androgen receptor signaling in prostate cancer development and progression. J. Carcinog. 10, 20. https://doi.org/10.4103/1477-3163.83937
- Lu, C., Wu, C., Ghoreishi, D., Chen, W., Wang, L., Damm, W., Ross, G.A., Dahlgren, M.K., Russell, E., Von Bargen, C.D., Abel, R., Friesner, R.A., Harder, E.D., 2021. OPLS4: improving force field accuracy on challenging regimes of chemical space. J. Chem. Theory Comput. 17 (7), 4291–4300. https://doi.org/10.1021/acs.jctc.1c00302.
- Maness, S.C., McDonnell, D.P., Gaido, K.W., 1998. Inhibition of androgen receptor-dependent transcriptional activity by DDT isomers and methoxychlor in HepG2 human hepatoma cells. Toxicol. Appl. Pharmacol. 151, 135–142. https://doi.org/10.1006/taap.1998.8431.
- Martinović, D., Dlake, L.S., Durhan, E.J., Greene, K.J., Kahl, M.D., Jensen, K.M., Makynen, E.A., Villeneuve, D.L., Ankley, G.T., 2008. Reproductive toxicity of vinclozolin in the fathead minnow: confirming an anti-androgenic mode of action. Environ. Toxicol. Chem. 27 (2), 478–488. https://doi.org/10.1897/07-206R.1.
- Matsumoto, T., Sakari, M., Okada, M., Yokoyama, A., Takahashi, S., Kouzmenko, A., Kato, S., 2013. The androgen receptor in health and disease. Annu. Rev. Physiol. 75, 201–224. https://doi.org/10.1146/annurev-physiol-030212-183656.
- Moilanen, A.-M., Riikonen, R., Oksala, R., Ravanti, L., Nykänen, P.S., Törmäkangas, O.P., Elo, T., 2015. Discovery of ODM-201, a new-generation androgen receptor inhibitor targeting resistance mechanisms to androgen signaling-directed prostate cancer therapies. Sci. Rep. 5, 12007. https://doi.org/10.1038/srep12007.
- Negreira, N., Rodríguez, I., Ramil, M., Rubí, E., Cela, R., 2009. Solid-phase extraction followed by liquid chromatography-tandem mass spectrometry for the determination of hydroxylated benzophenone UV absorbers in environmental water samples. Anal. Chin. Acta 654 (2), 162–170. https://doi.org/10.1016/j.aca.2009.09.033.
- OECD, 2018. Revised Guidance Document 150 on Standardised Test Guidelines for Evaluating Chemicals for Endocrine Disruption, OECD Series on Testing and Assessment, No. 150, OECD Publishing, Paris. doi: 10.1787/9789264304741-en.
- OECD, 2023. Test No. 458: Stably Transfected Human Androgen Receptor Transcriptional Activation Assay for Detection of Androgenic Agonist and Antagonist

- Activity of Chemicals, OECD Guidelines for the Testing of Chemicals, Section 4, OECD Publishing, Paris. doi: 10.1787/9789264264366-en.
- Olugbogi, E.A., Arobadade, O.A., Bodun, D.S., Omoseeye, S.D., Omirin, E.S., Fapohunda, O., Ekun, O.E., Metibemu, D.S., Shodehinde, S.A., Saliu, J.A., Omotuyi, O.I., 2024. Identification of apposite antagonist for androgen receptor in prostate cancer: an in silico study of fenugreek compounds. J. Biomol. Struct. Dyn. 42 (23), 12918–12934. https://doi.org/10.1080/07391102.2023.2273988.
- Park, Y., Jung, D.W., Milcamp, A., Takeyoshi, M., Jacobs, M.N., Houck, K.A., Ono, A., Bovee, T.F.H., Browne, P., Delrue, N., Kang, Y.S., Lee, H.S., 2021. Characterisation and validation of an *in vitro* transactivation assay based on the 22Rv1/MMTV\_GR-KO cell line to detect human androgen receptor agonists and antagonists. Food Chem. Toxicol. 152, 112206. https://doi.org/10.1016/j.fct.2021.112206.
- Pathak, R.K., Jung, D.W., Shin, S.H., Ryu, B.Y., Lee, H.S., Kim, J.M., 2024. Deciphering the mechanisms and interactions of the endocrine disruptor bisphenol a and its analogs with the androgen receptor. J. Hazard. Mater. 469, 133935. https://doi.org/ 10.1016/j.jhazmat.2024.133935.
- Rodil, R., Quintana, J.B., Concha-Graña, E., López-Mahía, P., Muniategui-Lorenzo, S., Prada-Rodríguez, D., 2012. Emerging pollutants in sewage, surface and drinking water in Galicia (NW Spain). Chemosphere 86 (10), 1040–1049. https://doi.org/ 10.1016/j.chemosphere.2011.11.053.
- Roy, A.K., Lavrovsky, Y., Song, C.S., Chen, S., Jung, M.H., Velu, N.K., Bi, B.Y., Chatterjee, B., 1999. Regulation of androgen action. Vitam. Horm. 55, 309–352. https://doi.org/10.1016/s0083-6729(08)60938-3
- Sakkiah, S., Ng, H.W., Tong, W., Hong, H., 2016. Structures of androgen receptor bound with ligands: advancing understanding of biological functions and drug discovery. Exp. Opin. Ther. Targets 20 (10), 1267–1282. https://doi.org/10.1080/ 14728222.2016.1192131.
- Sakkiah, S., Kusko, R., Pan, B., Guo, W., Ge, W., Tong, W., Hong, H., 2018. Structural changes due to antagonist binding in ligand binding pocket of androgen receptor elucidated through molecular dynamics simulations. Front. Pharmacol. 9, 492. https://doi.org/10.3389/fphar.2018.00492.
- Satoh, K., Nagai, F., Aoki, N., 2001. Several environmental pollutants have binding affinities for both androgen receptor and estrogen receptor α. J. Health Sci. 47 (5), 495–501
- Scsukova, S., Rollerova, E., Bujnakova Mlynarcikova, A., 2016. Impact of endocrine disrupting chemicals on onset and development of female reproductive disorders and hormone-related cancer. Reprod. Biol. 16 (4), 243–254. https://doi.org/10.1016/j. repbio.2016.09.001.
- Schreurs, R., Lanser, P., Seinen, W., van der Burg, B., 2002. Estrogenic activity of UV filters determined by an in vitro reporter gene assay and an in vivo transgenic

- zebrafish assay. Arch. Toxicol. 76 (5–6), 257–261. https://doi.org/10.1007/s00204-002-0348-4.
- Schrödinger Release, 2023-4. Schrödinger, LLC, New York, NY. <a href="https://www.schrodinger.com/life-science/download/release-notes/release-2023-4">https://www.schrodinger.com/life-science/download/release-notes/release-2023-4</a>.
- Schrödinger, L.L.C., 2024. What are the default settings for receptor grid generation in Glide? Schrödinger Knowledge Base, Article ID: 1842. <a href="https://www.schrodinger.com/kb/1842">https://www.schrodinger.com/kb/1842</a> (Accessed April 24, 2025).
- Serçinoğlu, O., Bereketoglu, C., Olsson, P.E., Pradhan, A., 2021. In silico and in vitro assessment of androgen receptor antagonists. Comput. Biol. Chem. 92, 107490. https://doi.org/10.1016/j.compbiolchem.2021.107490.
- Shtivelman, E., Beer, T.M., Evans, C.P., 2014. Molecular pathways and targets in prostate cancer. Oncotarget. 5 (17), 7217–7259. https://doi.org/10.18632/oncotarget.2406.
- Sifakis, S., Androutsopoulos, V.P., Tsatsakis, A.M., Spandidos, D.A., 2017. Human exposure to endocrine disrupting chemicals: effects on the male and female reproductive systems. Environ. Toxicol. Pharmacol. 51, 56–70. https://doi.org/ 10.1016/j.etap.2017.02.024.
- Skakkebaek, N.E., 2016. A brief review of the link between environment and male reproductive health: lessons from studies of testicular germ cell cancer. Horm. Res. Paediatr. 86 (4), 240–246. https://doi.org/10.1159/000443400.
- Tan, M.H., Li, J., Xu, H.E., Melcher, K., Yong, E.L., 2015. Androgen receptor: structure, role in prostate cancer and drug discovery. Acta. Pharmacol. Sin. 36 (1), 3–23. https://doi.org/10.1038/aps.2014.18.
- Wahl, J., Smieško, M., 2018. Endocrine disruption at the androgen receptor: employing molecular dynamics and docking for improved virtual screening and toxicity prediction. Int. J. Mol. Sci. 19 (6), 1784. https://doi.org/10.3390/ijms19061784.
- Xie, Y., Tian, Y., Zhang, Y., Zhang, Z., Chen, R., Li, M., Tang, J., Bian, J., Li, Z., Xu, X., 2022. Overview of the development of selective androgen receptor modulators (SARMs) as pharmacological treatment for osteoporosis (1998–2021). Eur. J. Med. Chem. 230, 114119. https://doi.org/10.1016/j.ejmech.2022.114119.
- Yamasaki, K., Takeoshi, M., Sawaki, M., Imatanaka, N., Shinoda, K., Takatsuki, M., 2003. Immature rat uterotrophic assay of 18 chemicals and Hershberger assay of 30 chemicals. Toxicology 183 (1–3), 93–115. https://doi.org/10.1016/s0300-483x(02) 00445-6.
- Yazdani, B., Sirous, H., Brogi, S., Calderone, V., 2023. Structure-based high-throughput virtual screening and molecular dynamics simulation for the discovery of novel SARS-CoV-2 NSP3 Mac1 domain inhibitors. Viruses. 15 (12), 2291. https://doi.org/ 10.3390/v15122291.
- Zacharia, L.C., 2017. Permitted daily exposure of the androgen receptor antagonist flutamide. Toxicol. Sci. 159 (2), 279–289. https://doi.org/10.1093/toxsci/kfx135.